C60/Collapsed Carbon Nanotube Hybrids: A Variant of Peapods

Hamid Reza Barzegar,[†,‡] Eduardo Gracia-Espino,[‡,#] Aiming Yan,[†,§,‖] Claudia Ojeda-Aristizabal,[†,§,‖] Gabriel Dunn,[†,§,‖] Thomas Wågberg,[‡] and Alex Zettl*,[†,§,‖,⊥]

[†]Department of Physics and [‖]Center of Integrated Nanomechanical Systems, University of California, Berkeley, California 94720, United States

[‡]Department of Physics, [#]Department of Chemistry, Umea University, 90187 Umea, Sweden

[§]Materials Sciences Division, Lawrence Berkeley National Laboratory, Berkeley, California 94720, United States

[⊥]Kavli Energy NanoSciences Institute at the University of California, Berkeley and the Lawrence Berkeley National Laboratory, Berkeley, California 94720, United States

S Supporting Information

ABSTRACT: We examine a variant of so-called carbon nanotube peapods by packing C_{60} molecules inside the open edge ducts of collapsed carbon nanotubes. C_{60} insertion is accomplished through a facile single-step solution-based process. Theoretical modeling is used to evaluate favorable low-energy structural configurations. Overfilling of the collapsed tubes allows infiltration of C_{60} over the full cross-section of the tubes and consequent partial or complete reinflation, yielding few-wall, large diameter cylindrical nanotubes packed with crystalline C_{60} solid cores.
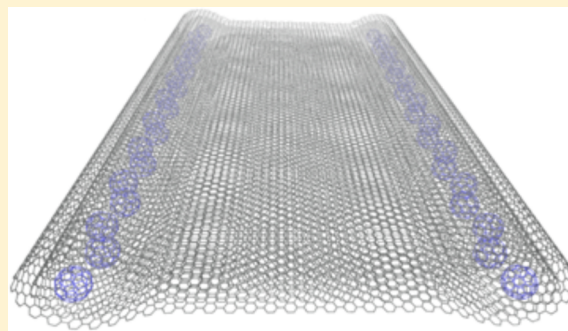
KEYWORDS: Peapods, fullerenes, collapsed carbon nanotubes, silocrystals

Hybrid nanostructures are of great interest due to the potential for engineering new materials with tunable physical and chemical properties. An example is the so-called nanotube "peapod" first described by Smith et al.,[1] where fullerene C_{60} molecules are encapsulated within single-wall carbon nanotubes (SWCNTs). Similar peapods have been produced using double and multiwalled CNTs[2,3] and boron nitride nanotubes.[4] Hornbaker et al.[5] experimentally showed that the molecular orbitals of encapsulated C_{60} in peapods modify the electronic band structure of SWCNTs, while some theoretical studies indicate a weak interaction between C_{60} and SWCNTs.[6−8] C_{60} inserted into nanotubes with larger inner diameter can assume a rather unusual packing structure.[2,4,9,10]

Flattened, collapsed carbon nanotubes (CCNTs), first reported by Chopra et al.[11] in 1995, are an interesting derivative of CNTs. It has been theoretically shown that CNTs are prone to collapse into a nearly flat, ribbon-like configuration if the diameter of the tube is larger than a critical diameter, which is an increasing function of number of tube walls.[11−13] The collapse may be induced by mechanical perturbation or, for sufficiently large diameter tubes, by thermal fluctuations. CCNTs represent the original realization of (bilayer or higher layer number) graphene nanoribbons[14,15] with perfectly bonded edge-atoms.[16] Importantly, the strain energy of the curved edges (which opposes the attractive van der Waals forces of the opposing graphene sheets) leads to open channels or ducts which run along the two edges of the CCNT. These

ducts, which are teardrop- or bulb-shaped in cross-section, are suitable for foreign species insertion, but the resulting hybrid CCNT/C_{60} systems have received relatively little attention.[17] Recently Wang et al.[18] showed that it is possible to insert C_{60} molecules in the duct of CCNT through a vapor transport process. Here we more extensively examine, experimentally and theoretically, hybrid CCNT/C_{60} systems. Although the hybrid structure has obvious similarities to conventional carbon nanotube peapods, there are key differences. First, the C_{60}s pack initially along the flattened tube edges and not in the tube center, and the noncylindrical teardrop shape of the CCNT edge ducts provides a different geometrical constraint for C_{60} packing; second, the modest van der Waals energy of the graphene layers allows some "ungluing" of the layers to accommodate differing amounts of C_{60} and thus also vastly different CCNT cross-section (the strong hoop strength afforded by the sp^2 bonds of uncollapsed CNTs prevents such "intercalation" flexibility); and third, the intrinsic band structure of CCNTs differs from that of CNTs, hence hybridization with the C_{60} molecules will be different from that encountered in conventional peapods. The new hybrid material makes it possible to combine the unique properties of C_{60} and rounded-edge graphene nanoribbons.

We first consider the anticipated ease for C_{60} insertion into a CCNT. Figure 1 schematically shows on the left a C_{60} molecule
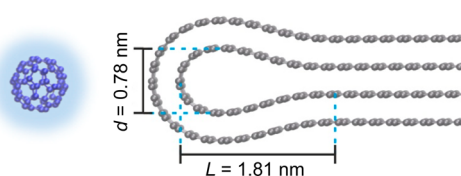

Figure 1. Precursor materials for C_{60}/CCNT hybrids. Left: An isolated C_{60} molecule, with diameter (carbon center to carbon center) 0.7 nm. The van der Waals interaction diameter (shadow) is somewhat larger at ~1 nm. Right: Cross-section of edge of fully collapsed two-walled CNT. A simple continuum elasticity model predicts a duct bulb height $d = 0.78$ nm and duct width $L = 1.81$ nm. Unless the duct bulb size increases (via C_{60}-induced partial ungluing of the collapsed CNT), the C_{60} does not fit inside the duct.

which has a carbon-center to carbon-center distance of 0.7 nm and a more relevant van der Waals outer diameter of ~1.0 nm.[2] The two-walled CCNT shown on the right side of Figure 1 has, using a simple continuum elasticity model, a duct bulb height $d = 0.78$ nm and bulb width $L = 1.81$ nm.

If CCNTs were completely rigid, it would be extremely difficult to insert C_{60} into the edge ducts, as the C_{60} is simply too big for the duct size. A related observation is that insertion of C_{60} in large diameter *uncollapsed* SWCNT is exothermic,[2] while it is strongly endothermic for SWCNTs with a diameter smaller than 1.25 nm; for small diameter tubes C_{60} insertion requires stretching of the SWCNT wall and is thus energetically unfavorable.[19] Table 1 displays the calculated dimensions of the

Table 1. Theoretically and Experimentally Determined Width L and Inner Height d of Unfilled CCNT with Different Number of Walls

CCNT n	theoretical calculation		experiment	
	L (nm)	d (nm)	L (nm)	d (nm)
$n = 1$	1.65	0.71		
$n = 2$	1.81	0.78		
$n = 3$	1.99	0.86		
$n = 4$	2.19	1.03	2.5	0.94

duct bulb cross-section for single- to four-walled CCNTs. The results indicate that d and L values slightly increase from single- to four-walled CCNTs. However, even for a four-walled CCNT, the d value is smaller than the threshold diameter for C_{60} insertion. For comparison available experimental data are also presented in the table.

Importantly, however, the open ducts of CCNTs are fundamentally very different from the central cylindrical hollow of uncollapsed CNTs. The opposite walls in a CCNT are attracted to each other only by the graphitic inter layer binding energy (of order of 50 meV per atom)[20] which allows ungluing of the edges of the core flattened region and swelling of the duct cross-section during C_{60} insertion (the C_{60} molecules have a higher binding energy with the graphitic layers compared to the interlayer binding of graphite).[11] This flexibility allows the CCNT edge ducts to readily accept single or even multiple chains of C_{60}. In a sense, the CCNT is a deformable medium and readily accepts and conforms to suitable inserted foreign species.

We now discuss experimental synthesis, transmission electron microscopy (TEM) characterization, and theoretical analysis of the hybrid C_{60}/CCNT structures. We employ highly crystalline arc-grown MWCNTs, either produced in house or obtained commercially, whose end we remove by thermal oxidation. One to few-wall, relatively large inner diameter CCNTs are then obtained by sonication of the MWCNTs, which removes some of the core tubes in a telescoping fashion and collapses the remaining outer walls[21] (more experimental data on CCNTs are presented in Supporting Information). Filling of the CCNT ducts with C_{60} is also performed in solution,[22−24] either in a separate subsequent sonication step (following first drying of the CCNTs to ensure removal of residual trapped solvent) or, more directly, in concert with the core extraction/collapse sonication process. We choose to insert C_{60} using a solution[25,26] rather than vapor transport[18,27,28] process as the former has been shown to an effective lower temperature, a much faster method to create conventional peapods. In addition solution based lowers entanglement and/or bundling of CCNTs, which in turn facilitate the ungluing of opposite walls in the CCNTs. We also choose n-hexane as a solvent in which, due to low solubility, C_{60} molecules form clusters instead of discrete solvated molecules. The direct interaction of C_{60} clusters and CCNTs results in effective filling of CCNTs.[29] For the one-step collapsing/filling method, C_{60} and uncapped MWCNTs are dispersed in hexane and sonicated for 2 h using an ultrasonic probe. During sonication the temperature of the dispersion increases up to 80 °C due to mechanical energy transfer from the sonicator. We find that the elevated temperature is a key factor for effective filling.[25] During the sonication process hexane lost to evaporation is replenished to ensure a consistent concentration of C_{60} and CCNTs. Different initial C_{60} concentrations yield different levels of duct filling, as discussed in detail below. See the Methods section for additional synthesis details. A statistical analysis of the TEM images taken from different parts of the TEM grid reveals that at optimum filling condition up to 70% of the CCNTs can be filled by different configurations of C_{60} molecules.

Figure 2A(i) shows a TEM image of the edge region of a two-walled CCNT into which C_{60} has been inserted. A chain-like row of C_{60} molecules can be clearly seen near the inner edge of collapsed tube ribbon. This and many related images recorded for different C_{60}/CCNT orientations (see Supporting Information) clearly show that the C_{60}s are situated in the open ducts near the curved edges of the collapsed tube.

The $C_{60}−C_{60}$ center-to-center distance along straight chain segments in the CCNT ducts is experimentally found (on average) to be 0.98 nm, in accord with the 1 nm spacing reported for conventional CNT peapods.[1] Figure 2A(ii) and (iii) represents our theoretical results for a linear chain of C_{60}s within the ducts of a two-walled CCNT. C_{60} insertion has increased the bulb height and width significantly (compare to Figure 1): d increases from 0.78 to 1.32 nm and L increases from 1.81 to 2.18 nm. Not surprisingly, our calculated value of d for CCNTs with a linear chain of C_{60}'s is close to the threshold diameter (1.25 nm) for encapsulating C_{60} in SWCNTs.[19,30] The predicted $C_{60}−C_{60}$ distance in the linear chain in our calculations is 0.97 nm, consistent with experiment. It should be noted, however, that our simulations show that the strictly linear chain of C_{60}s is not particularly stable: the tendency is for the C_{60}s to open the bulb up even more and assume a staggered configuration (thereby increasing
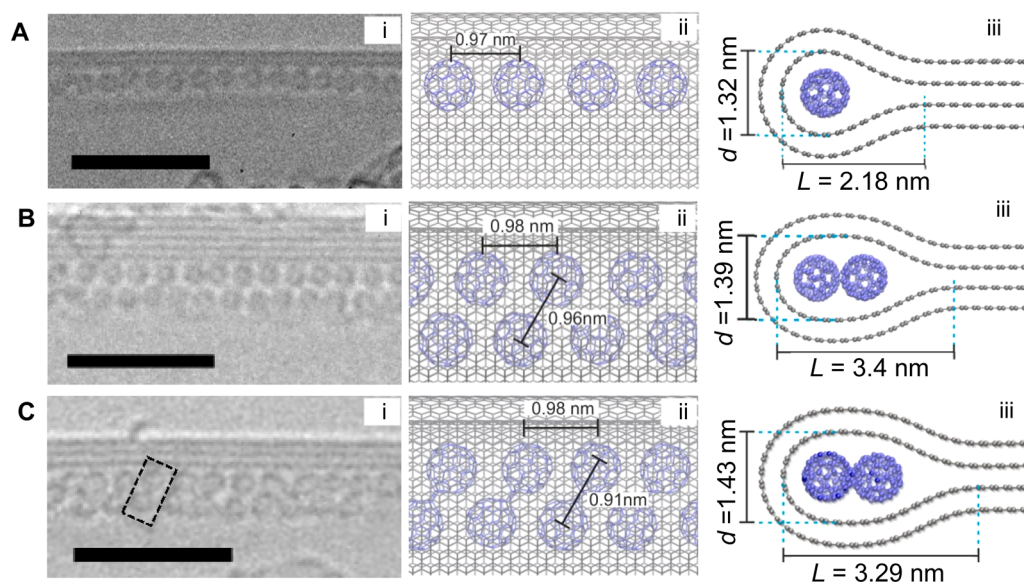
Figure 2. High-resolution TEM image and theoretical modeling (top view and duct cross section) of (A) a double-wall CCNT filled with a linear chain of C_{60} molecules. (B) A five-walled CCNT filled with staggered C_{60} configuration. (C) A three-walled CCNT showing C_{60} dimers, a result of C_{60} close packing in a stagger configuration plus duct pressure combined with elevated temperature and/or electron beam stimulation. Dashed box in C(i) indicates a C_{60} pair forming dimers. Calculated values for dimensions of the bulb, L and d, and $C_{60}-C_{60}$ distance are indicated in the image. Note that for better comparison of duct cross section dimensions the result for double-walled CCNTs are presented in the image. The scale bar in all experimental images is 5 nm.
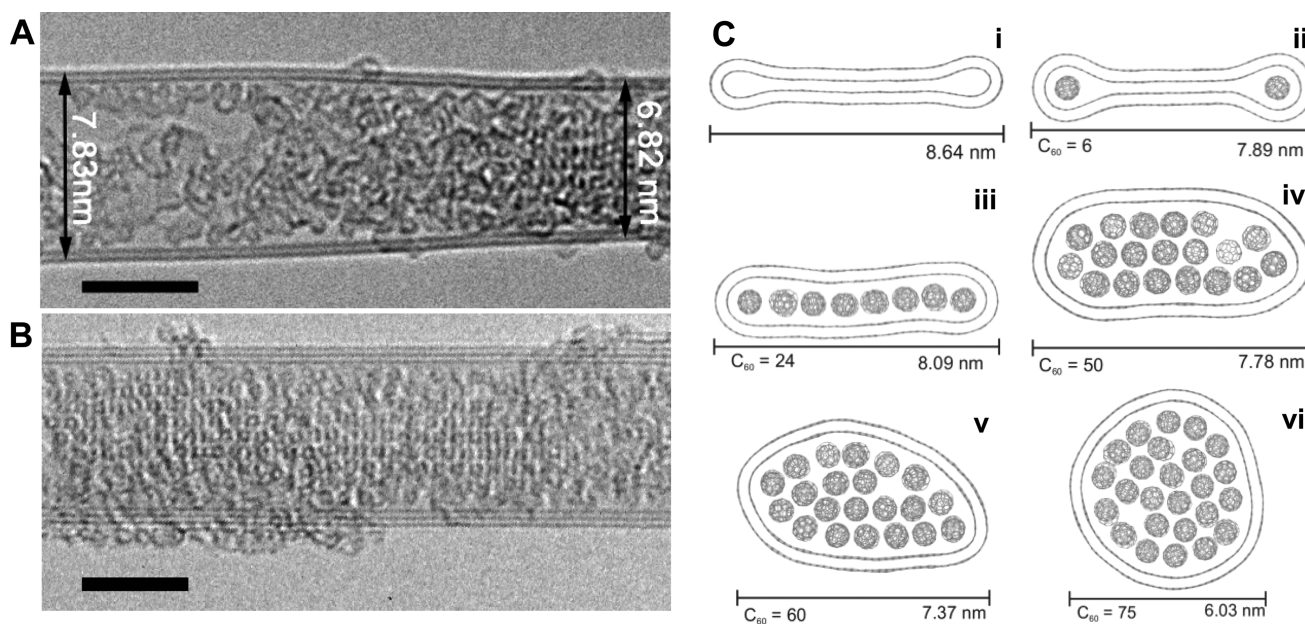

Figure 3. High-resolution TEM image of (A) a double-walled CCNTs in intermediate stage of reinflating. (B) A completely reinflated three-walled CCNT. (C) Modeling for change in width of a double-walled CCNT with diameter close to the one in the figure (A); (i) to (vi) different stages of filling/reinflation after the structures are relaxed at 300 K. The main change in the width of CCNT happens when the C_{60} molecules form a three-dimensional structure. Note that the width of CCNT with single layer C_{60} increases compared to the CCNT with linear chains of C_{60}'s. Scale bars: (A and B) 5 nm.

the overall C_{60} density). Indeed, this is observed experimentally, as exemplified in Figure 2B.

By increasing the concentration of C_{60} during the solution based synthesis, the filling of ducts can be enhanced and the linear chain overwhelmed. Figure 2B(i) shows a five-wall CCNT edge where the duct has widened, and the inserted C_{60}s have assumed a staggered configuration. Figure 2B(ii) and (iii) show corresponding model calculations for staggered C_{60}s in two-wall CCNT (for simplicity and better comparison of duct

cross section dimensions, all the model calculations presented in Figure 2 are for a two-walled tube—the wall number does not change the results substantively; see Table 1). The C_{60}'s are close-packed in the duct, which (see Figure 2B(iii)) has an increased width $L = 3.4$ nm to now accommodate the "double row" of C_{60}s. Such a staggered packing of C_{60} molecules has been observed in CNT peapods and in filled BN tubes with diameters of 2 nm,[2,4] but there the staggered chains tend to spiral along the axis of the tubes, whereas for CCNTs ducts the

helical degree of freedom is quenched. We remark that we have also observed C_{60}-filled CCNTs, where regions of nearly linear chain configurations coexist end-to-end in the same duct with regions of staggered chains, and we have also observed staggered chains in single-walled CCNT. All of these observations support that the C_{60} configuration at the duct is independent of number of walls (see Supporting Information).

C_{60}'s stagger-packed into CCNT ducts experience anisotropic confinement pressure from the duct walls. As can be readily seen in the cross-section model views (iii) in Figure 2, C_{60}'s situated closer to the central axis of the CCNT tend to be pushed toward the edge by the collapsed graphene layers. The close-packing and enhanced pressure leads to distortions in the zigzag staggered chain and sets the stage for C_{60}–C_{60} dimerization. Evidence for compressed C_{60} chains in a two-walled CCNT is presented in Figure 2C(i), where experimentally the C_{60}-C_{60} distance along the duct axis is 0.98 nm, while the angled C_{60}–C_{60} pair distance is 0.90 nm. A representative pair is outlined by the dashed box in Figure 2C(i). Such pairs likely represent well-known C_{60} dimerization,[31–34] easily induced in the CCNT case by duct pressure combined with elevated temperature and/or electron beam stimulation; it is realized via the so-called 2 + 2 cycloaddition resulting from the breaking of two double bonds of neighboring C_{60} molecules. Our model calculations for the dimerized C_{60}/CCNT case are shown in Figure 2C(ii) and (iii) (The results of similar model calculations for single- to four-walled CCNT are presented in Supporting Information, Table S1). It should be noted that although the value of L increases with increasing the wall number (see Table 1) due to the teardrop shape of the cross section (d is decreasing along L), the C_{60} molecules are always (independent of number of walls) pushed toward the edges by the collapsed gaphene layer.

An interesting question is whether the C_{60} insertion process into CCNTs is self-limiting (at say the staggered chain level) or if it continues unchecked as long as sufficient C_{60} is available and the ducts remain free of foreign matter. We find strong evidence that, with sufficient C_{60} concentration in the preparation solution and sonication time, C_{60} insertion can continue until the CCNT is fully "reinflated" to a circular cross-section; the CNT has then a completely filled crystalline C_{60} core.

Figure 3 shows CCNTs at different stages of this overfilling and reinflation process. Figure 3A shows a TEM image over the full width of a CCNT (the contamination debris seen is likely predominantly on the outer surface of the tube). In the left part of the image, C_{60}'s are observed in the two duct regions, forming incomplete linear chains. On the right side of the image, C_{60} span the entire interior width of the tube; here the outer projected width of the tube is also reduced. Considering the width of the flattened left part, and accounting for the curvature of the ducts, the host tube here has a fully inflated diameter of approximately 5.8 nm, giving evidence that the right part of the tube is not yet completely circular and is still reinflating. Figure 3C shows a simple modeling—using molecular dynamic after relaxation at 300 K—for a double-walled CCNT at different steps (3 Ci to 3Cvi) of reinflation, in which certain number of C_{60} molecules (presented below each image) are encapsulated in a supercell containing 12 unit cells of the examined CCNT (the starting configurations of Figure 3C at $T = 0$ K are presented in Figure S6). It is clear from the figures that if a CCNT fills with a single (two-dimensional) layer of C_{60} molecules (Ciii) its diameter slightly increases

compared to C_{60}/CCNT with a linear chain (Cii) configuration. Thus, the decrease in diameter of the CCNT (on the right side of the image) reveals that the CCNT contains a three-dimensional crystal of C_{60} rather than a monolayer sheet. A comparison between the final C_{60}/CCNTs configuration, presented in Figure 3C, and the starting configuration (at $T = 0$ K, see Figure S6) indicates that the encapsulated C_{60} molecules rearranged after relaxing the structure at 300 K and form more crystalline structure rather than an amorphous configuration. Figure 3B shows a different CCNT apparently completely filled with C_{60}. This is the ultimate limit of C_{60} packing—the core of the reinflated, cylindrical CNT is completely filled with crystalline C_{60}. We note also that the tube in Figure 3B has a diameter of 10 nm which is above the calculated critical diameter for a three-walled tube.[12,35]

The reinflation of CCNT is further supported by tilting a C_{60}/CCNT around its axis in a TEM experiment. Figure 4A
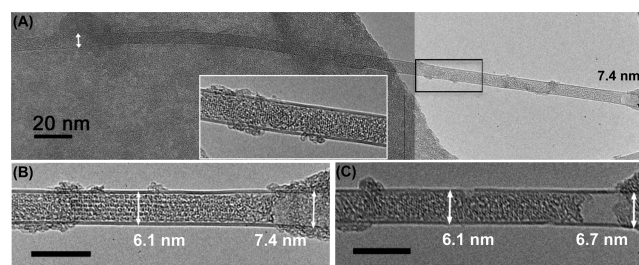

Figure 4. TEM image of (A) a double-walled CCNT reinflated by C_{60} insertion. The image is a combination of three TEM images along the length of the tube and shows a high degree of filling. The arrows in the upper image show the parts of the C_{60}/CCNT where there are gaps between C_{60} molecules. This section of the tube possesses a larger width, indicating that tube was collapsed before C_{60} insertion. The inset in (A) shows high magnification image of the middle part (shown by rectangle). Higher magnification images of the right side of the tube (B) before and (C) after tilting the tube by 20° around the tube axis. Scale bars: 10 nm.

shows TEM images of a double-walled CCNT reinflated by C_{60} insertion in which C_{60} molecules are packed along its length except in two regions where there are gaps between C_{60} filling (indicated by arrows). The wider diameter of the CCNT in the empty regions (7.4 nm) compared to the reinflated parts (6.1 nm) indicates that the tube was collapsed before C_{60} insertion. The inset shows high magnification image of the middle part (indicated by rectangle). Figure 4B,C shows the right section of the same tube before and after the tube is tilted around its axis by about 20°, respectively. After tilting the projection image of the empty region, with a nearly flat structure, is narrowed (6.7 nm) compared to the one before tilting (7.4 nm). In contrast, as shown in Figure 4B,C, the middle part of the tube displays no change in diameter, strongly supporting a full reinflation. A simple modeling indicating change in the diameter of an empty CCNT and a half-full reinflated CCNT is presented in Figure S4. Additional TEM images of reinflated tubes before and after tilting are also presented in Supporting Information (Figure S5). Interestingly, the constraint of a partially reinflated CCNT is fundamentally different from the cylindrical constraint of a fully inflated tube, allowing an even richer family of structures than afforded by silocrystals.[4,36,37]

Methods. *Sample Preparation and Characterization.* The caps of highly crystalline arc discharge grown MWCNTs (either produced in house[11] or obtained commercially; MER

Corporation), are first removed by thermal oxidation for 30 min, using a TGA furnace (TGA7; PerkinElmer), at 700 °C in an argon/oxygen (ratio of 1:4) environment (which typically results in a mass loss of 50%). Extraction of inner walls of uncapped CNTs and C_{60} intercalation in CCNTs are performed either in a single step or in separate sonication steps. In the first approach the heat-treated MWCNTs are mixed with C_{60} (99.9%; MER Corporation) with mass ratio 1:1 or 1:3. Thereafter the C_{60}/MWCNTs mixture is dispersed in hexane (with a C_{60} concentration of 0.3 mg/mL) using an ultrasonic sonicator (Sonics; with a 3 mm probe) for 1−3 h. The amount of solvent is tracked during sonication, and fresh solvent is added as necessary. The sample is then collected by filtration, using a PTFE filter with a pore size of 0.45 μm, and washed by toluene to remove the free C_{60} molecules from the surface of CCNTs. The collected material is dispersed in 1% weight per volume solution of sodium dodecyl sulfate (SDS, Sigma-Aldrich 99%) in water and sonicated for 30 min. The dispersion is centrifuged for 1 h at 20 000g. The supernatant is mixed with methanol, and the precipitated material is collected. In the second approach the uncapped CNTs are first dispersed in 1% weight per volume solution of SDS in water and sonicated for 1 h to synthesis CCNTs. The CCNTs are then separated by centrifugation and filtration followed by overnight heat treatment in a vacuum oven at 200 °C to remove the residual solvent in the CCNTs. The insertion of C_{60} in CCNTs is performed in the same manner described above by dispersing and sonication of the mixture of CCNT and C_{60} in hexane.

Following solution synthesis, the C_{60}-filled CCNT samples are dried and then dispersed on TEM grids using 1,2-dichloromethane, followed by a 2 h heat treatment in a vacuum oven at 200 °C. High-resolution TEM imaging is performed using a JEOL 2010 (with a LaB_6 gun) operated at 80 keV.

Computational Methodology. Molecular dynamics (MD) simulations are performed using the large-scale atomic/molecular massively parallel simulator (LAMMPS).[38] The interatomic interactions are characterized by the adaptive intermolecular reactive empirical bond order (AIREBO) potential.[39] The AIREBO potential consists of the reactive empirical bond order (REBO) term[40] for short-range interactions ($r < 2$ Å), a Lennard−Jones term defining long-range van der Waals interaction ($2 < r < 10.2$ Å), and a torsion term describing diverse dihedral angle preferences.

The CCNTs are built by considering an armchair (n,n) configuration, where the consecutive layers are created with a chirality of $(n + 5, n + 5)$ with respect to the previous layer (interlayer distance ~3.4 Å). Then, four different systems are created (from 1 up to 4-walls) where 12 unit cells are considered in order to avoid self-interactions. The C_{60} filled CCNTs are simulated by introducing 12 C_{60} molecules at both edges of the CCNT. The MD simulations are performed under periodic boundary conditions, and the intercell separation is kept at 30 nm to avoid lateral interactions. A constant temperature of 0 K is ensured during the simulation to eliminate the atomic vibration. The molecular dynamics (MD) simulation is carried out under a constant number of atoms and volume, the temperature is controlled by a Berendsen thermostat with a 1 ps damping constant. The temperature is increased by a constant rate equal to 3.0 K/ps up to 298 K; subsequently, the MD simulation is continued for another 800 ps using a time step of 1 fs.

ASSOCIATED CONTENT

⑤ Supporting Information

Information, TEM characterization of CCNTs and C_{60}/CCNTs, and theoretical modeling calculation. This material is available free of charge via the Internet at http://pubs.acs.org.

AUTHOR INFORMATION

Corresponding Author

*E-mail: azettl@berkeley.edu.

Author Contributions

H.R.B., T.W., and A.Z. conceived the experiment; E.G.E. performed the theoretical modeling; G.D. contributed to CNT synthesis; A.Y. contributed to TEM imaging; C.O.A. contributed to C_{60} processing; H.R.B. performed the experiments and TEM measurements; H.R.B. and A.Z. wrote the manuscript; all authors discussed the results and commented on the manuscript.

Notes

The authors declare no competing financial interest.

REFERENCES

(1) Smith, B. W.; Monthioux, M.; Luzzi, D. E. *Nature* **1998**, *396* (6709), 323−324.

(2) Khlobystov, A. N.; Britz, D. A.; Ardavan, A.; Briggs, G. A. D. *Phys. Rev. Lett.* **2004**, *92* (24), 245507.

(3) Frohlich, T.; Scharff, P.; Schliefke, W.; Romanus, H.; Gupta, V.; Siegmund, C.; Ambacher, O.; Spiess, L. *Carbon* **2004**, *42* (12−13), 2759−2762.

(4) Mickelson, W.; Aloni, S.; Han, W. Q.; Cumings, J.; Zettl, A. *Science* **2003**, *300* (5618), 467−469.

(5) Hornbaker, D. J.; Kahng, S. J.; Misra, S.; Smith, B. W.; Johnson, A. T.; Mele, E. J.; Luzzi, D. E.; Yazdani, A. *Science* **2002**, *295* (5556), 828−831.

(6) Liu, X.; Pichler, T.; Knupfer, M.; Golden, M. S.; Fink, J.; Kataura, H.; Achiba, Y.; Hirahara, K.; Iijima, S. *Phys. Rev. B* **2002**, *65* (4), 045419.

(7) Yoon, Y. G.; Mazzoni, M. S. C.; Louie, S. G. *Appl. Phys. Lett.* **2003**, *83* (25), 5217−5219.

(8) Utko, P.; Nygard, J.; Monthioux, M.; Noe, L. *Appl. Phys. Lett.* **2006**, *89* (23), 233118.

(9) Hodak, M.; Girifalco, L. A. *Phys. Rev. B* **2003**, *67* (7), 075419.

(10) Spudat, C.; Meyer, C.; Goss, K.; Schneider, C. M. *Phys. Status Solidi B: Basic Solid State Phys.* **2009**, *246* (11−12), 2498−2501.

(11) Chopra, N. G.; Benedict, L. X.; Crespi, V. H.; Cohen, M. L.; Louie, S. G.; Zettl, A. *Nature* **1995**, *377* (6545), 135−138.

(12) Benedict, L. X.; Chopra, N. G.; Cohen, M. L.; Zettl, A.; Louie, S. G.; Crespi, V. H. *Chem. Phys. Lett.* **1998**, *286* (5−6), 490−496.

(13) He, M.; Dong, J.; Zhang, K.; Ding, F.; Jiang, H.; Loiseau, A.; Lehtonen, J.; Kauppinen, E. I. *ACS Nano* **2014**, *8* (9), 9657−9663.

(14) Li, X.; Wang, X.; Zhang, L.; Lee, S.; Dai, H. *Science* **2008**, *319* (5867), 1229−1232.

(15) Son, Y.-W.; Cohen, M. L.; Louie, S. G. *Nature* **2006**, *444* (7117), 347−349.

(16) Li, Y. F. *Phys. Chem. Chem. Phys.* **2014**, *16* (5), 1921−1929.

(17) Fan, J.; Yudasaka, M.; Yuge, R.; Futaba, D. N.; Hata, K.; Iijima, S. *Carbon* **2007**, *45* (4), 722−726.

(18) Wang, Q.; Kitaura, R.; Yamamoto, Y.; Arai, S.; Shinohara, H. *Nano Res.* **2014**, *7* (12), 1843−1848.

(19) Rochefort, A. *Phys. Rev. B* **2003**, *67* (11), 115401.

(20) Gobre, V. V.; Tkatchenko, A. *Nat. Commun.* **2013**, No. 4, 2341.

(21) Choi, D. H.; Wang, Q.; Azuma, Y.; Majima, Y.; Warner, J. H.; Miyata, Y.; Shinohara, H.; Kitaura, R. *Sci. Rep-Uk* **2013**, No. 3, 1617.

(22) Yudasaka, M.; Ajima, K.; Suenaga, K.; Ichihashi, T.; Hashimoto, A.; Iijima, S. *Chem. Phys. Lett.* **2003**, *380* (1−2), 42−46.

(23) Khlobystov, A. N.; Britz, D. A.; Wang, J.; O'Neil, S. A.; Poliakoff, M.; Briggs, G. A. D. *J. Mater. Chem.* **2004**, *14* (19), 2852−2857.

(24) Noe, L.; Monthioux, M. Liquid phase synthesis of "peapods" at room temperature. In *International Conference on Carbon "Carbon'04*, Ext. Abstract (CD-ROM), Oral/C105, **2004**.

(25) Simon, F.; Kuzmany, H.; Rauf, H.; Pichler, T.; Bernardi, J.; Peterlik, H.; Korecz, L.; Fulop, F.; Janossy, A. *Chem. Phys. Lett.* **2004**, *383* (3−4), 362−367.

(26) Simon, F.; Peterlik, H.; Pfeiffer, R.; Bernardi, J.; Kuzmany, H. *Chem. Phys. Lett.* **2007**, *445* (4−6), 288−292.

(27) Smith, B. W.; Luzzi, D. E. *Chem. Phys. Lett.* **2000**, *321* (1−2), 169−174.

(28) Kim, K.; Lee, Z.; Malone, B. D.; Chan, K. T.; Aleman, B.; Regan, W.; Gannett, W.; Crommie, M. F.; Cohen, M. L.; Zettl, A. *Phys. Rev. B* **2011**, *83* (24), 245433.

(29) Chamberlain, T. W.; Popov, A. M.; Knizhnik, A. A.; Samoilov, G. E.; Khlobystov, A. N. *ACS Nano* **2010**, *4* (9), 5203−5210.

(30) Bandow, S.; Takizawa, M.; Kato, H.; Okazaki, T.; Shinohara, H.; Iijima, S. *Chem. Phys. Lett.* **2001**, *347* (1−3), 23−28.

(31) Moret, R.; Launois, P.; Wagberg, T.; Sundqvist, B.; Agafonov, V.; Davydov, V. A.; Rakhmanina, A. V. *Eur. Phys. J. B* **2004**, *37* (1), 25−37.

(32) Sundqvist, B. Polymeric fullerene phases formed under pressure. In *Fullerene-Based Materials: Structures and Properties*; Prassides, K., Ed.; Springer-Verlag: Berlin, 2004; Vol. *109*, pp 85−126.

(33) Smith, B. W.; Monthioux, M.; Luzzi, D. E. *Chem. Phys. Lett.* **1999**, *315* (1−2), 31−36.

(34) Han, S. W.; Yoon, M.; Berber, S.; Park, N.; Osawa, E.; Ihm, J.; Tomanek, D. *Phys. Rev. B* **2004**, *70* (11), 113402.

(35) Xiao, J.; Liu, B.; Huang, Y.; Zuo, J.; Hwang, K. C.; Yu, M. F. *Nanotechnology* **2007**, *18* (39), 395703.

(36) Mughal, A.; Chan, H. K.; Weaire, D. *Phys. Rev. Lett.* **2011**, *106* (12), 1.

(37) Hirahara, K.; Suenaga, K.; Bandow, S.; Kato, H.; Okazaki, T.; Shinohara, H.; Iijima, S. *Phys. Rev. Lett.* **2000**, *85* (25), 5384−5387.

(38) Plimpton, S. *J. Comput. Phys.* **1995**, *117* (1), 1−19.

(39) Stuart, S. J.; Tutein, A. B.; Harrison, J. A. *J. Chem. Phys.* **2000**, *112* (14), 6472−6486.

(40) Brenner, D. W.; Shenderova, O. A.; Harrison, J. A.; Stuart, S. J.; Ni, B.; Sinnott, S. B. *J. Phys.: Condens. Matter* **2002**, *14* (4), 783−802.